

POLITECNICO DI TORINO  
Repository ISTITUZIONALE

Minimum-Propellant Direct, Assisted, and Slingshot Return Trajectories from Mars, Jupiter, and their moons

*Original*

Minimum-Propellant Direct, Assisted, and Slingshot Return Trajectories from Mars, Jupiter, and their moons / Patti, A., Mascolo, L., Battipede, M.. - (2023). (74th International Astronautical Congress (IAC) Baku (AZE) 2-6 October 2023).

*Availability:*

This version is available at: 11583/3002052 since: 2025-07-23T17:25:24Z

*Publisher:*

International Astronautical Federation

*Published*

DOI:

*Terms of use:*

This article is made available under terms and conditions as specified in the corresponding bibliographic description in the repository

*Publisher copyright*

IAC/IAF postprint versione editoriale/Version of Record

Manuscript presented at the 74th International Astronautical Congress (IAC), Baku (AZE), 2023. Copyright by IAF

(Article begins on next page)

IAC-23-78764

## Minimum-Propellant Direct, Assisted, and Slingshot Return Trajectories from Mars, Jupiter, and their moons.

Alessio Patti<sup>a\*</sup>, Luigi Mascolo<sup>b</sup>, Manuela Battipede<sup>c</sup>

<sup>a</sup> Politecnico di Torino, Italy, alessio.patti@studenti.polito.it

<sup>b</sup> Politecnico di Torino, Italy, luigi.mascolo@polito.it

<sup>c</sup> Politecnico di Torino, Italy, manuela.battipede@polito.it

### Abstract

For future space missions, exploiting a planet's moons to escape from its sphere of influence can significantly improve the performance of the mission itself. In fact, being able to return to Earth while saving the maximum amount of propellant possible allows us, at the preliminary stage, to design the mission with more mass to be allocated to the payload, which means being able to carry out more detailed explorations that will allow us to gain a greater understanding of our planetary system.

This study focuses on identifying the minimum-propellant mission architectures for future return missions from planets with moons to Earth. In particular, Mars and Jupiter are selected as the central bodies, and their moons, including Phobos, Deimos, and the four most massive moons of Jupiter, are taken into consideration.

The analysis explores various escape strategies, such as direct escape trajectories from each gravitational body and either gravity assists or powered flybys. The study considers more than 100 different mission architectures, which include direct escape trajectories and all the possible permutations with one or two additional moons. A detailed analysis narrows the search space for the best gravitational body combinations and identifies the most promising candidate strategies for escape. Different dynamical models are implemented, including a three-body dynamical model and a bi-circular four-body problem, respectively for when one or two moons are considered along with the more massive primary. The heliocentric phase follows Keplerian motion and is patched to the escape conditions from the primaries at the sphere of influence. JPL's DE432s ephemerides are implemented to retrieve the celestial bodies' states over time.

A Lambert's problem for the return trajectory explores launch windows between January 1, 2025, and December 31, 2050. Results show significant differences between the Mars and Jupiter frameworks, with an evident cut-off convenience threshold for considering moons to escape when a bigger primary to smaller primary flyby is implemented. In contrast, solutions that exploit trajectories from a smaller primary towards the bigger one to take advantage of its gravitational pull or the Oberth effect are promising regardless of the specific primary's mass ratio. Notably, the solutions exhibit periodicity over the years due to the combined planetary ephemerides.

**Keywords:** escape trajectories; flyby; genetic algorithm; four-body-problem;

### Acronyms/Abbreviations

- Planar Bicircular Restricted 4-Body Problem (PBR4BP)
- Circular Restricted 3-Body Problem (CR3BP)
- Sphere Of Influence (SOI)
- Equation of Motion (EOM)
- Fly-By Phobos (FBPh)
- Fly-By Deimos (FBDe)
- Best Direct Escape (BDE)
- Best Combined Fly-by (BCFB)
- Distance Unit (DU)
- Velocity Unit (VU)

### 1. Introduction

The possibility of being able to reach Mars in the near future is becoming more and more concrete especially in recent years. The difficulties in accomplishing such a mission are not only related to how to get to the red planet, but, if we want to get human beings there, we also have to pose the problem of how to get the astronauts safely back to Earth.

The work presented in this paper aims to identify the best possible maneuver that will allow a space probe located on a low Martian orbit to return to Earth while consuming the least amount of propellant. Therefore, to achieve this, a four-body planar bicircular model (BCR4BP) will be used to evaluate whether and how fruitful, via flyby

maneuvers, a planet's satellites can actually be an advantage.

Therefore, four different types of maneuvers will be presented: a direct escape, an assisted escape by flyby of Phobos, an assisted escape by flyby of Deimos, and finally, a combined flyby maneuver with both Mars satellites will also be evaluated.

The analyses performed in this paper should not be understood to apply only to the Mars-Phobos-Deimos tertiary system; rather, a parametric study was conducted in which as the gravitational parameter of the binary system and the distance between the secondary and tertiary body vary, it is possible to describe all existing three-body systems.

In fact, since Phobos and Deimos are very small and not very massive satellites, it would be possible to conclude, even before results are obtained, that their gravitational aids to the probe are actually negligible; for this reason, the parametric study consists of simulating, in steps of an order of magnitude each, an increase in the gravitational parameter of the binary system, so that it is possible to investigate what the minimum mass ratio between primary and secondary must be in order for it to make sense to speak of a gain of at least 1 m/s over the  $\Delta V$  that is needed to implement a direct escape maneuver without exploiting the gravitational assistance of a planet's satellites.

Therefore, in the first chapter the aim is to briefly summarize the purpose of this work so as to provide a general overview and the logical flow followed. The second chapter will describe the dynamic model implemented, namely a four-body planar bicircular model (PBR4BP), with all the quantities that characterize it. In order to consistently describe this four-body model, a code was implemented in the Matlab environment: the core of this code is a genetic algorithm that will be described and analyzed in the third chapter. Its purpose is to find the best possible combination of initial conditions that, integrated over time according to the EOMs of the PBR4BP, allow minimizing the errors defined as constraints imposed on the final conditions. The results obtained will be explained and commented on in the fourth chapter while in the fifth and last chapter will present the final conclusions.

## 2. Dynamic Model

In order to evaluate as consistently as possible the possible flyby maneuvers that a generic S/C can perform by exploiting the gravitational effects of the satellites of the general planet in the solar system, it is appropriate to introduce a model in which account is taken of the fact that there are three bodies in question that can significantly influence the trajectory of a spacecraft, such a model is the Planar Bicircular Restricted 4 Body Problem (BCR4BP).

The model analyzed in this section is the BCR4BP which describes the motion of an infinite mass (P3) under the influence of three massive bodies: the Earth (P1), the Moon (P2) and the Sun (P4). Obviously, it will suffice to change the binary gravitational parameters of the two main bodies involved and the distance between the secondary and tertiary body to fit this model on any other systems centered in the various planets of the solar system, so that the interaction that the two main satellites of the single planet analyzed will have on the final trajectory described by the S/C can be evaluated. In this model, the Earth and Moon move in circular paths around their mutual barycenters, denoted in the figure 1 by B1. Similarly, the Sun and B1 move in Keplerian circular motion around their mutual barycenter B2.

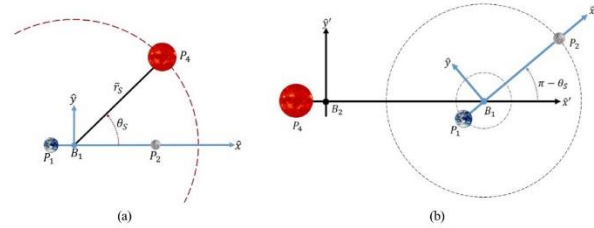


**Figure 1.** Rotating Earth-Moon system (a) and rotating Sun-B1 system (b).

Note that the BCR4BP is a time-dependent system in which the position of the Sun in the Earth-Moon rotation frame is defined by a single angle called  $\theta_s$ . The Sun moves clockwise around B1 (i.e., the angle  $\theta_s$  is negative), as illustrated in Figure 1(a); this effect is due to the fact that the Earth-Moon system centered in B1 rotates with a unit angular velocity in accordance with the definition of the CR3BP, while the Sun, rotating in turn around this rotating system will have a smaller angular velocity so that there will be this apparently clockwise circular motion.

The equations of motion describing the motion of the assumed massless particle (P3), in the rotating Earth-Moon system, are described below:

$$\ddot{x} = 2\dot{y} + \frac{\partial Y}{\partial x}$$

$$\ddot{y} = -2\dot{x} + \frac{\partial Y}{\partial y}$$

$$\ddot{z} = \frac{\partial Y}{\partial z}$$

where  $Y$  is the pseudo-potential in the rotating Earth-Moon system and is defined as:

$$Y = \frac{1-\mu}{r_{13}} + \frac{\mu}{r_{23}} + \frac{x^2 + y^2}{2} + \varepsilon \left( \frac{m_4}{r_{43}} - \frac{m_4}{a_4^3} (x_4x + y_4y + z_4z) \right)$$

where  $x_i, y_i$  and  $z_i$  are the components of the position of the point  $P_i$  with respect to the barycenter of the rotating Earth-Moon reference system,  $\mu$  is the gravitational parameter of the Earth-Moon system,  $r_{ij}$  is the modulus of the position of  $P_i$  with respect to  $P_j$ ,  $m_4$  is the dimensionless mass of the fourth body  $P_4$  defined as  $\frac{m_4}{m_1+m_2}$ , and  $a_4$  is the semi-major axis of the circular orbit traveled by the Sun around the barycenter B1. The  $\varepsilon$  term is a scaling parameter for the Sun's mass:  $\varepsilon = 0$  reflects a restricted circular three-body problem CR3BP without solar gravity, while  $\varepsilon = 1$  represents the BCR4BP. Just as in CR3BP it is advantageous to study the motion of the satellite in the synodic system, similarly in this case it is advantageous to study the equations of motion in the rotating Sun-B1 system: in this reference system the positive direction of the x-axis is directed from the Sun to the Earth-Moon barycenter B1, the positive direction of the z-axis is defined as the direction of the angular momentum of the Sun-B1 orbit, and the positive direction of the y-axis completes the triad. The rotating Sun-B1 system is illustrated in the figure 1(b). In this particular case, the four-body model was applied to the Mars-Phobos-Deimos ternary system: the fundamental parameters that govern the evolution of EOMs once initial conditions are fixed are:

1. The gravitational parameter  $\mu$  of the binary system:

$$\mu = \frac{\mu_{Ph}}{\mu_{Ma} + \mu_{Ph}} = 1.6606e-8$$

2. The unit distance, that is, the distance between primary and secondary by which all other distances involved will be dimensionalized:

$$DU = 9378 \text{ km}$$

3. The unit velocity, that is, the tangential velocity with which the secondary body moves in its circular orbit of unit radius around Mars and by which all other velocities involved will be dimensionalized:

$$VU = \sqrt{\frac{\mu_{Ma} + \mu_{Ph}}{DU}} = 2.1370 \text{ km/s}$$

4. The dimensionless mass of the tertiary body;

$$m_{De} = \frac{M_{De}}{M_{De} + M_{Ma}} = 0.0313$$

5. The dimensionless distance between the secondary and the tertiary (the distance between the primary and secondary is always fixed and unitary);

$$\rho_{De} = \frac{\rho_{MD}}{DU} = 2.5015$$

6. The angular velocity of the secondary;

$$\omega_{Ph} = \sqrt{\frac{\mu_{Ma} + \mu_{Ph}}{DU^3}} = 2.2788e-4 \text{ rad/s}$$

7. The angular velocity of the tertiary;

$$\omega_{De} = \sqrt{\frac{\mu_{Ma} + \mu_{Ph}}{\rho_{MD}^3}} = 5.8073e-5 \text{ rad/s}$$

8. The angular position from which the tertiary body starts  $\theta_{De}$ ;

Specifically, the parametric study conducted involves varying from a minimum value of 1.6606e-8, which represents the value of the real gravitational parameter in the case of the Mars-Phobos system, to a maximum value of 1.6606e-1.

Note that, for example, in the case of the Jupiter-Ganymede binary system (which represents the most massive of Jupiter's many moons) the gravitational parameter  $\mu$  is worth 7.7065e-5, while in the more common case of the Earth-Moon binary system it is worth 0,0122, which is why, this parametric analysis should not be seen as descriptive only of the Mars-Phobos binary system, but on the contrary, the Mars-Phobos system represents only one of the possible combinations of optimization of the gravitational parameter, which, varying in the range just described, allows to describe any binary system in the solar system. The upper limit is due to the fact that it has been shown that it is useless to talk about a generic binary system if the mass ratios are greater than 1/4, otherwise the system will not be self-stable.

The code provides the possibility of being able to parametrically set the distance between the secondary and tertiary as well, so that any ternary system can be analyzed, since the distance between the primary and secondary will always be fixed and unity. In particular, the study was conducted by setting a dimensionless length range between the secondary and tertiary between 1 and 3: in this way it was possible to incorporate within the analysis the real cases of both the Mars-Phobos-Deimos tertiary system, characterized by a distance of 2,5015 between Phobos and Deimos, as well as the case of the tertiary Jupiter-Ganymede-Callisto system characterized by a distance between secondary and tertiary equal to 1,7589.

On the choice of the distance between secondary and tertiary will depend the value of the angular velocity possessed by the tertiary itself, while, with regard to the value of the angular position possessed by the tertiary body at the initial instant, a further analysis was conducted aimed at measuring how many launch windows are possible within a year. In fact, assuming that we want to analyze the specific case of Mars-Phobos-Deimos in the synodic system described by PBR4BP it will be necessary to impose that the angle  $\theta_{Ph}$  describing the angular position of Phobos along its circular orbit is always zero (by definition of a synodic system), so, the only variable that one could choose to vary would be the angle  $\theta_{De}$  describing the angular position of Deimos in its circular orbit.

In reality, however, from the point of view of the synodic system, what matters is the variable  $\Delta\theta$  defined as  $\theta_{De} - \theta_{Ph}$  because when this variable cancels out (i.e., when Phobos and Deimos are along the same line joining) it will mean that it will be possible to have a launch window.

For this reason, a study was first conducted to measure how many times during the course of a year the  $\Delta\theta = 0$  situation occurs: the results are shown in Graph 2, which illustrates that, defined by the angular velocities of Phobos and Deimos, the optimal phasing condition occurs 855 in a year, i.e., more than twice a day.

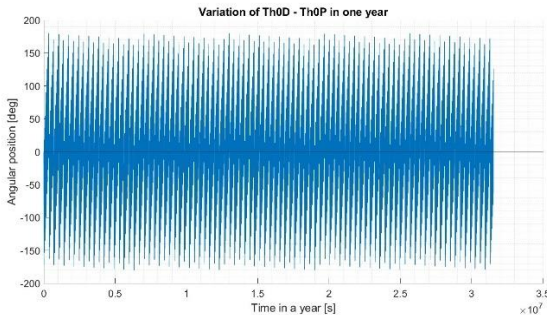


**Figure 2.** Optimal phasing conditions

In this way it is possible to justify the hypothesis, which will be adopted in the course of the present work, of optimal phasing, for the trajectories that will be shown in the fourth chapter.

### 3. Genetic algorithm

Once the initial conditions have been established, they must in fact be propagated over time, following the EOMs of the PBR4BP, so as to arrive at the final conditions on which the two constraints in terms of position and velocity described above must be imposed.

The genetic algorithm implemented consists of generating a population of 1000 individuals, each of which will be formed by 5 properties that are called genes (or alleles) and that represent the variables involved as a initial conditions, in order they are:

1. The  $\Delta\mathbf{V}$  as the first gene, that is, the impulse that is given at the initial instant that is to be added vectorially (the  $\Delta\mathbf{V}$  will be given tangentially) to the circular velocity possessed by the S/C, which, being on an LMO orbit of altitude  $h = 400$  km will have a tangential velocity equal to:

$$V_c = \sqrt{\frac{\mu_{Ma} + \mu_{Ph}}{R_{Ma} + h}} = 3.3620 \text{ km/s}$$

2. the angle in the synodic plane  $\theta$  as the second, i.e., the angular distance with respect to the x-axis of the Mars-Phobos synodic system at which the S/C is located at the time the impulse is given. This parameter can be changed from  $0^\circ$  to  $360^\circ$  and in this way it is possible to simulate the start of the trajectory at any of the positions occupied by the satellite along its circular orbit in LMO;
3. the angle outside the synodic plane  $\phi$  as the third. This angle has been made to explore freely between  $0^\circ$  and  $360^\circ$  but, for each trajectory implemented, the genetic algorithm has converged to the condition  $\phi = 0$ , which is the one of interest, since, having implemented a planar model, the aim is precisely to simulate a trajectory that is as planar as possible, going to minimize the  $\Delta\mathbf{V}$  with respect to the nonplanar case;
4. the dimensionless time  $\mathbf{tf}$  taken by the S/C to go from the starting point to the ending point, as well as the integration time as the last gene. For example, a dimensionless time equal to  $2\pi$  means that the trajectory will have been integrated for a period of time equal to the amount of time it takes Phobos to make a complete rotation of  $360^\circ$  around Mars, that is, about 7 hours and 39 minutes;
5. The  $\Delta\Theta$  as the fifth and last gene. This parameter is defined as the difference between, respectively, the angular position possessed by Deimos  $\theta_{De}$  and Phobos  $\theta_{Ph}$  at the initial instant and is of fundamental importance since the synodic system is a rotating system with angular velocity equal to that possessed by Phobos, which is why it is defined with  $\theta_{Ph} = 0$  at any

instant in time. By setting this variable with values between 0° to 360° it will therefore be possible to describe the relative position of Deimos in its circular orbit around Mars, as well as to go to identify the possible launch windows that will occur at the value  $\Delta\Theta = 0$ , that is, when the two Mars satellites are along the same conjunction.

These variables will thus determine what will be the random initial conditions that will be propagated by the genetic algorithm and, from this point on, the trajectory followed by the satellite will be uniquely defined. To propagate the orbit in time, the ode113 function of Matlab was used, which allows solving differential equations by giving as input the initial conditions and integration time. Once the vector containing the probe positions of the various time steps, output of integration with ode113, has been obtained, it is possible to impose constraints on the final position and velocity that the S/C will have to reach the boundaries of the Mars SOI with the right velocity, so as to enter with exactly  $V_{1H}$  on the Hohmann transfer and begin its heliocentric phase that will bring the probe of back to Earth. Thus, the difference between the final position reached after integration and the target radius ( $r_{SOI}$ ) and between the final velocity possessed by the S/C and the target velocity ( $V_{1H}$ ) represent errors: the goal of the genetic algorithm is precisely to find the best individual that minimizes these errors.

Specifically, in the genetic algorithm implemented in this thesis work, it was fixed:

- a 50% probability of having a random mutation of one of the fifth genes in an individual,
- a probability of 30% of having a mutation by algebraic sum, i.e., that offspring are generated by an algebraic sum of the parents' alleles (this solution helps to narrow down the search for the optimal solution more and more as if it were a true bisection method).
- a 70% probability of having a crossover, that is, that the offspring inherit one or more random genes from the father and the rest of the genes from the mother.

In addition, it was also chosen to generate 1/4 of new random population at each generation both to have a well-distributed population avoiding the presence of similar individuals, and also because this allows the algorithm to be able to explore other parts of the universe

in terms of combinations of the 5 parameters, so that it will be able to get out of a local minimum by evolving toward another local minimum perhaps characterized by a smaller error in absolute value. In addition to keeping track of the error, the genetic algorithm is structured to plot, at each generation, the 5 alleles of the best individual according to the order  $[\Delta V, \theta, \varphi, t_f, \Delta\theta]$  and the various errors that the final conditions (which are obtained by propagating the initial conditions defined by these 5 parameters) will have with respect to the target conditions, according to the following order:

- **err1**: represents the dimensionless difference between the norm of the vector containing the information about the final radius reached by the S/C and the norm of the target radius vector defined as  $\frac{r_{SOI}}{DU}$ . Having an err1  $\rightarrow 0$  means that we have arrived at the boundaries of the SOI of Mars;
- **err2**: represents the dimensionless difference between the norm of the vector containing the information about the final velocity reached by the S/C and the  $V_{\infty}$ . To also have an err2  $\rightarrow 0$  is to have arrived at the boundaries of the SOI of Mars with exactly the modulus of the velocity it takes to make the Hohmann ellipse and return to Earth.

Finally, the variable **err** will be defined as the sum of these two errors and will represent the main parameter to be tended to zero by the genetic algorithm.

#### 4. Results

This chapter will report the results obtained through the modeling of the Mars-Phobos-Deimos Mars-Phobos system in the Matlab environment and the implementation of the genetic algorithm analyzed in the chapter 3. The trajectories that will be analyzed will be classified into four different categories:

1. Direct hyperbolic escape maneuvers;
2. Assisted escape maneuvers through the flyby of Phobos;
3. Assisted escape maneuvers through the flyby of Deimos;
4. Assisted escape maneuvers through the combined flyby of Phobos and Deimos.

The results will be presented both in graphical form through the appropriate plots and in schematic form through the tables 1 and 2 that summarize, respectively, the optimal initial conditions that integrated over time allow for that particular trajectory and the errors in terms of the position vector ( $err1$ ) and modulus ( $err2$ ) of the velocity vector.

In the plots, the dimensions of Mars are those actually possessed by the red planet (only dimensionalized with respect to DU) while the dimensions of Phobos and Deimos were voluntarily increased to make their positions visible during trajectory propagation.

#### 4.1 Best Direct Escape

As can be visualized of the plots in Figure 3 as well as from the table 1, the optimal direct escape trajectory is obtained by providing a  $\Delta V$  of 1,2036 km/s in the tangential direction when the S/C is at an angular distance of 231,54°.

The trajectory has a dimensionless duration equal to the time it takes Phobos to make a rotation of 48.054 radians around Mars; this means that, since Phobos has an angular velocity of equal to  $\omega_{ph}$ , it will take the probe 2,1088e5 sec to arrive at the SOI boundaries of Mars, which is about 58 hours and 48 minutes.

On the other hand, from the table 2 it is possible to visualize how well the genetic algorithm worked, we are in fact talking about an overall dimensionless error of the order of  $10e-10$  so it is possible to conclude that the trajectory described by the S/C will very accurately meet all the two constraints listed in chapter 3, representing a very reliable trajectory.

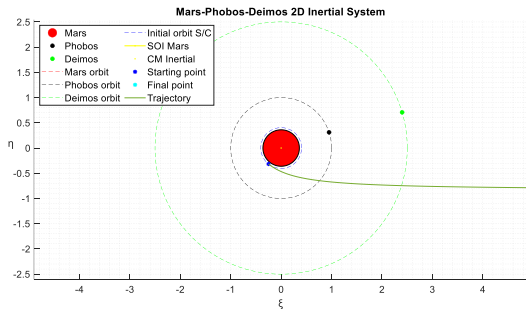


Figure 3. BDE Trajectory

Then in Figure 4, the velocity trend in the inertial system is shown both to allow a future comparison to be conducted with flyby maneuvers in which, instead, a velocity spike will be noted at the proximity to Phobos and/or Deimos, and to show how the velocity tends to move asymptotically toward the  $V_\infty$  value, a sign that the  $err2$  is very close to zero.

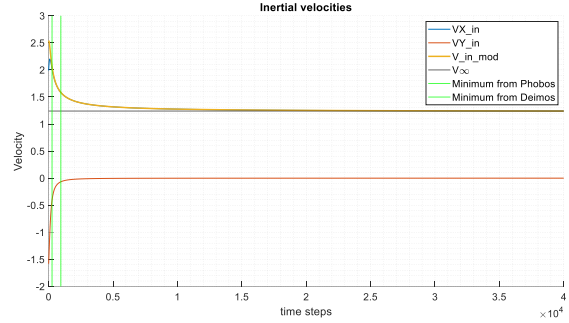


Figure 4. BDE Inertial velocities plot

For a complete understanding of the trajectory, Figure 5 also shows the energy trend of the trajectory followed by the S/C. In a two-body model, the energy of a trajectory remains constant; in this case, however, having implemented a four-body model, a perturbation can be expected, which, as shown by Figure 5, concerns the sixth decimal place (to give an example that is as concrete as possible, this is the same order of magnitude as the perturbative action that the Sun has toward a satellite that is at an Earth-Sun distance from the latter), demonstrating how microscopic Phobos and Deimos are and how their gravitational effects are insignificant but still measurable.

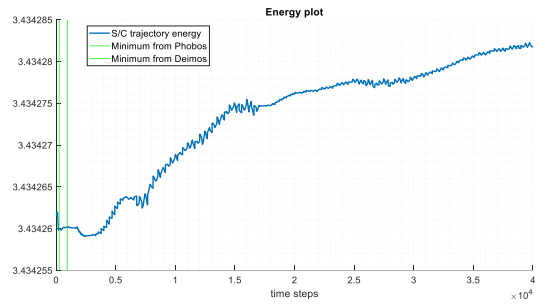


Figure 5. BDE Energy plot

#### 4.2 Best Phobos Flyby

In this subsection, the FBPh6 trajectory will be analyzed in detail, that is, the one that would occur if the Mars-Phobos binary system had a gravitational parameter 6 orders of magnitude greater than it real actually possessed. In particular, the FBPh6 maneuver makes it possible to arrive at the boundaries of the Mars SOI by spending a  $\Delta V$  of 0,6711 km/s compared to the 1,2036 km/s of the direct escape, which means a more than significant savings of about 0,53 km/s, implementing a flyby maneuver from behind with Phobos that will see it, at its point of minimum relative distance, approach Mars' satellite to a minimum distance of 357 km from its surface.

Also four subplots representing the Mars-Phobos-Deimos system "photographed" at different time instants are first shown: top left at the initial instant when the pulse is provided, top right at the temporal instant when the S/C has the shortest distance to Phobos, bottom left at the temporal instant when the S/C has the shortest distance to Deimos, and, finally, bottom right at the final instant when, that is, the S/C has reached the SOI of Mars. Next, a zoom of the trajectory is also depicted so that it is possible to visualize in detail how the trajectory followed by the probe is deflected due to the gravitational effect of Phobos.

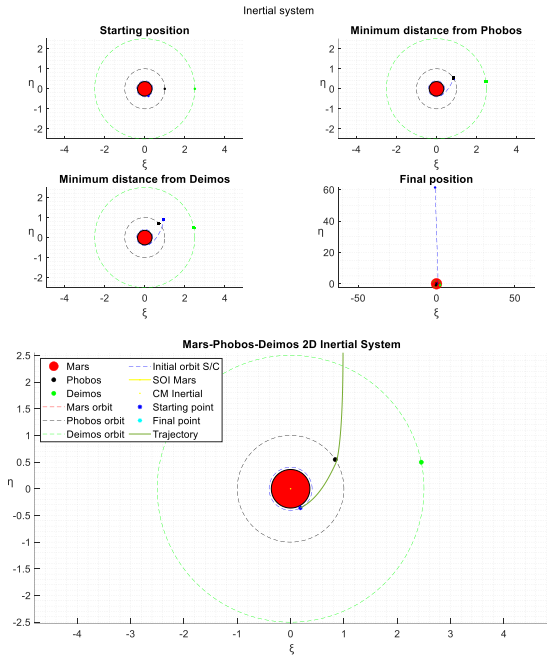


Figure 6. FBPh6 Trajectory

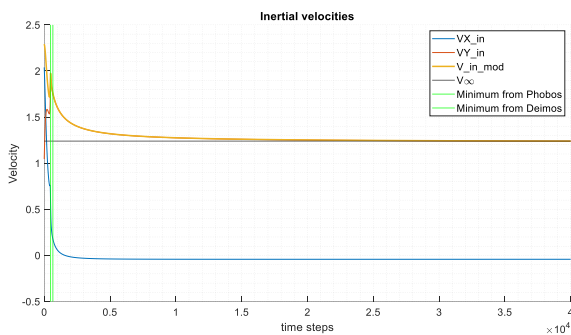


Figure 7. FBPh6 Inertial velocities plot

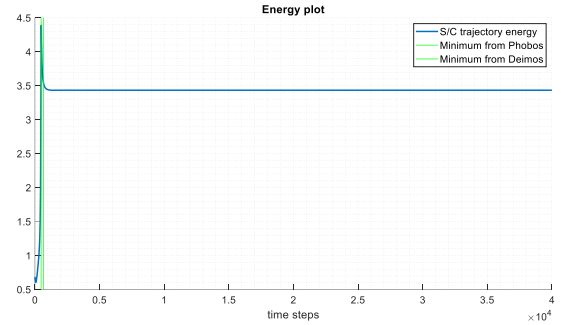


Figure 8. FBPh6 Energy plot

### 4.3 Best Deimos Flyby

As can be visualized from the table 1, the best possible case is implemented by giving an impulse in the tangential direction equal to 0,8032 km/s when the S/C is at an angular distance equal to 263,69°, allowing a savings in terms of  $\Delta V$  of about 0,4 km/s compared to the direct escape maneuver. This propellant savings is achieved at the expense of a slightly longer trajectory duration of 2,1766e5 s, i.e., about 60 hours and 26 minutes.

Specifically, again there will be a flyby of Deimos from behind in which the probe will arrive at a minimum distance of 503 km from the satellite's surface: this information, as well as in the case of the flyby of Phobos analyzed above, must however be taken with caution since we are analyzing a nonreal case in which, in order to visualize the gravitational effects of the Mars satellites we intentionally increase their mass so that the trajectory followed by the probe can actually be curved in the vicinity of their presence but no assumption has been made about the size in terms of radius that Phobos and Deimos should have as a result of having fictitiously acquired mass. Strictly speaking, in fact, one would have to specify that the minimum relative distances between the S/C and Phobos/Deimos (357 km and 503 km, respectively) refer, not so much to their surface, but to their center of mass, so logically these values should be subtracted from the value in kilometers in radius that Phobos and Deimos would have if they actually had a mass of 1,08e22 kg and 2e22 kg.

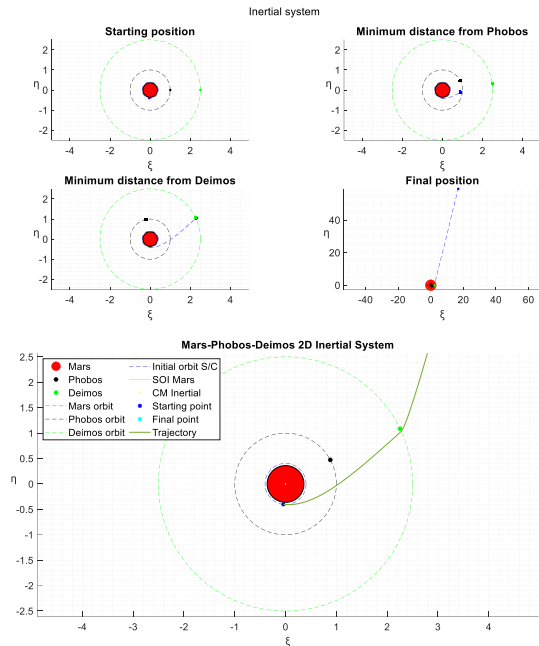


Figure 9. FBDe7 Trajectory

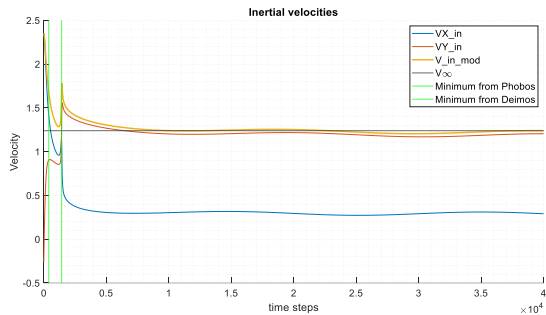


Figure 10. FBDe7 Inertial velocities plot

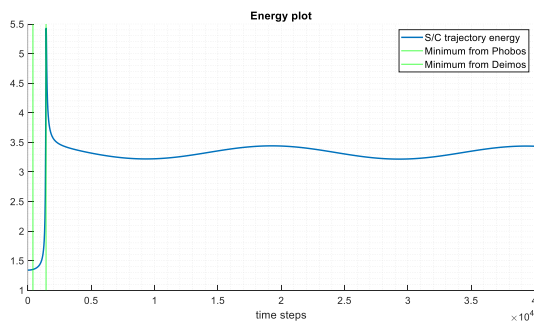


Figure 11. FBDe7 Energy plot

#### 4.4 Best Combined Flyby

In this subsection, the combined flyby maneuver with both of Mars' satellites is shown and analyzed. In order to implement this maneuver, an angle  $\theta_{Ph}$  equal to  $0^\circ$  and an angle  $\theta_{De}$  equal to  $61^\circ$  was imposed so that the trajectory followed by the S/C and curved by the Phobos flyby could also pass in the vicinity of Deimos. In addition, following the parametric study implemented for the individual flybys, it was decided to combine the FBPh6 and FBDe7 cases.

As can be visualized from the summary table 1 the optimal case is obtained by generating a tangential pulse equal to 0,6275 km/s when the S/C is at an angular position of  $298,61^\circ$ , with a gain of 0.5761 km/s compared with the case of direct escape without any gravitational assistance: the first flyby will take place from behind with Phobos greatly accelerating the probe as the latter will pass, at its point of minimum distance from the satellite, at a distance equal to 34 km from its surface (the closer the probe passes the attractor body, the more it will be accelerated for free); subsequently, the second flyby with Deimos will instead occur from in front, so in this case Deimos will decelerate the S/C, which, at its point of minimum distance, will be at a distance equal to 340 km from its surface.

The fact that this is a flyby first from behind to accelerate and then from in front to brake should not be surprising since the goal of the mission is not only to arrive at the boundaries of the SOI of Mars with any speed, but also to get there with the right velocity in terms of modulus (the direction of the velocity vector is instead automatically satisfied by the initial assumption of optimal phasing), which is why it is necessary for Deimos to slow down the S/C to allow it to arrive at the SOI with exactly the modulus of  $V_\infty$ .

To have a definitive proof of the flyby occurring, it can be seen from Figure 13 how flyby peaks in the velocity trend occur this time at the flyby of Phobos and Deimos, respectively. This double discontinuity is also found in terms of energy in Figure 14, an unmistakable sign of the interaction between the S/C and the moons of Mars.

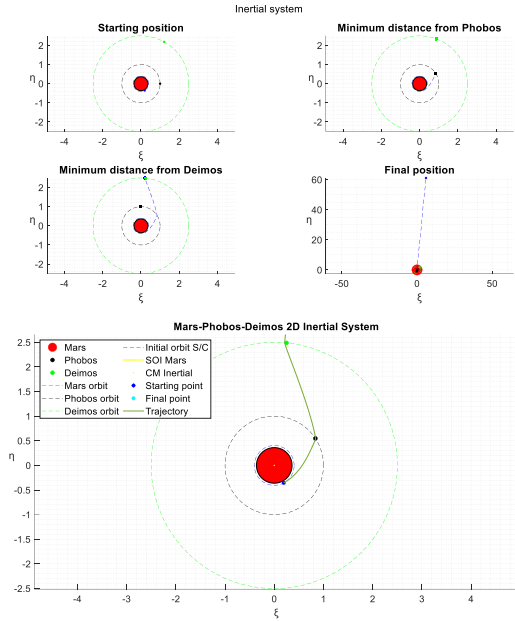


Figure 12. BCFB Trajectory

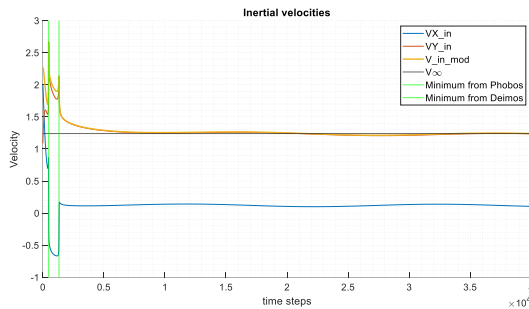


Figure 13. BCFB Inertial velocities plot

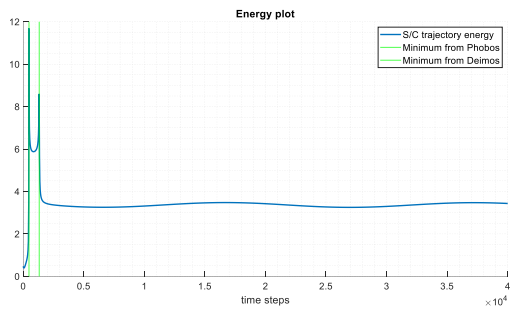


Figure 14. BCFB Energy plot

#### 4.5 Summary trajectories and final results

The following table summarizes in schematic form the results obtained. Specifically, a parametric analysis was conducted in which the gravitational parameter  $\mu$  of a generic binary system was varied from a minimum value of  $1,6606e-8$ , which represents the real case of the Mars-Phobos binary system, to a maximum value of  $1,6606e-1$ , with the purpose of going to investigate what the minimum binary gravitational ratio must be in order for it to make sense to talk about a gain of at least 1 m/s compared to the  $\Delta V$  that is needed instead to make a direct escape without any gravitational assistance from a planet's satellites. Note that, for example, in the case of the Jupiter-Ganymede binary system (which represents the most massive of Jupiter's many satellites) the gravitational parameter  $\mu$  is worth  $7,8065e-5$ , while in the more common case of the Earth-Moon binary system it is worth  $0,0122$ , which is why, this parametric analysis should not be seen as descriptive only of the Mars-Phobos binary system, but on the contrary, the Mars-Phobos system represents only one of the possible combinations of optimization of the gravitational parameter, which, varying in the range just described, allows to describe any binary system in the solar system. The upper limit is due to the fact that it has been shown that it is useless to talk about a generic binary system if the mass ratios are greater than  $1/4$ , otherwise the system will not be self-stable.

The code provides the possibility of being able to parametrically set the distance between the secondary and tertiary as well, so that any ternary system can be analyzed, since the distance between the primary and secondary will always be fixed and unity.

In particular, the study was conducted by setting a dimensionless length range between the secondary and tertiary between 1 and 3: in this way it was possible to incorporate within the analysis the real cases of both the Mars-Phobos-Deimos tertiary system, characterized by a distance of 2,5015 between Phobos and Deimos, as well as the case of the tertiary Jupiter-Ganymede-Callisto system characterized by a distance between secondary and tertiary equal to 1,7589.

In contrast, the table 2 shows the errors related to a trajectory. In particular, the column err refers to the dimensionless sum between err1 (which determines how accurately the S/C has arrived at the boundaries of Mars' SOI) and err2 (which determines how accurately the final velocity of the S/C is close to  $V_\infty$ ): as one can easily visualize these are very low errors, even negligible compared to the magnitudes involved. The second column, on the other hand, allows us to visualize the error on the final position expressed in a dimensional way, however: as can be seen we are talking about errors that in the worst case are of the order of 10 m, while as for the third column, which shows the error on the

velocity expressed in a dimensional way we have an error that in the worst case is of the order of 10 mm/s. This accuracy of the results is to be attributed to the robustness of the genetic algorithm described in Chapter 3, which allows for errors that are all the lower the more the number of generations performed is increased. In the specific case, these results were obtained by setting a number equal to 100 generations, where each generation consists of a population consisting of 1000 individuals.

Label	Trajectory [kg]	$\mu$ [/]	$\Delta V$ [km/s]	$\theta$ [deg]	$\varphi$ [deg]	$t_f$ [rad]
<b>BDE</b>	$M_{Ph}$ and $M_{De}$	$1,6606 \times 10^{-8}$	1,2036	231,54	0	48,054
FBPh0	$M_0 = M_{Ph}$	$1,6606 \times 10^{-8}$	1,2036	299,77	0	48,054
FBPh1	$M_1 = 10^1 \cdot M_{Ph}$	$1,6606 \times 10^{-7}$	1,2036	300,13	0	48,054
FBPh2	$M_2 = 10^2 \cdot M_{Ph}$	$1,6606 \times 10^{-6}$	1,2036	299,55	0	48,054
FBPh3	$M_3 = 10^3 \cdot M_{Ph}$	$1,6606 \times 10^{-5}$	1,2010	299,69	0	48,055
FBPh4	$M_4 = 10^4 \cdot M_{Ph}$	$1,6606 \times 10^{-4}$	1,1888	299,34	0	48,061
FBPh5	$M_5 = 10^5 \cdot M_{Ph}$	$1,6606 \times 10^{-3}$	1,0352	299,04	0	48,138
<b>FBPh6</b>	$M_6 = 10^6 \cdot M_{Ph}$	$1,6606 \times 10^{-2}$	0,6711	297,15	0	48,314
FBPh7	$M_7 = 10^7 \cdot M_{Ph}$	$1,6606 \times 10^{-1}$	0,1944	291,56	0	48,268
FBDe0	$M_0 = M_{De}$	$1,6606 \times 10^{-8}$	1,2036	269,91	0	48,054
FBDe1	$M_1 = 10^1 \cdot M_{De}$	$1,6606 \times 10^{-8}$	1,2036	270,59	0	48,054
FBDe2	$M_2 = 10^2 \cdot M_{De}$	$1,6606 \times 10^{-8}$	1,2036	269,74	0	48,054
FBDe3	$M_3 = 10^3 \cdot M_{De}$	$1,6606 \times 10^{-8}$	1,2036	269,84	0	48,054
FBDe4	$M_4 = 10^4 \cdot M_{De}$	$1,6606 \times 10^{-8}$	1,2029	269,64	0	48,055
FBDe5	$M_5 = 10^5 \cdot M_{De}$	$1,6606 \times 10^{-8}$	1,1928	269,77	0	48,074
FBDe6	$M_6 = 10^6 \cdot M_{De}$	$1,6606 \times 10^{-8}$	1,1452	268,85	0	48,197
<b>FBDe7</b>	$M_7 = 10^7 \cdot M_{De}$	$1,6606 \times 10^{-8}$	0,8032	263,69	0	49,599
<b>BCFB</b>	$M_{Ph}$ and $M_{De}$	$1,6606 \times 10^{-2}$	0,6275	298,61	0	48,518

**Tab 1.** Mars-Phobos-Deimos Martiocentric results.

Label	err [/]	err1 [mm]	err2 [mm/s]
<b>BDE</b>	$8,5413 \times 10^{-10}$	0,0179	0,0012
FBPh0	$9,3178 \times 10^{-9}$	12,3649	0,0171
FBPh1	$1,1113 \times 10^{-7}$	418,4932	0,1421
FBPh2	$3,4383 \times 10^{-6}$	$1,0667 \times 10^4$	4,9173
FBPh3	$6,9397 \times 10^{-6}$	$1,8829 \times 10^3$	14,4012
FBPh4	$2,5879 \times 10^{-7}$	219,0044	0,5031
FBPh5	$2,0811 \times 10^{-7}$	$1,8926 \times 10^3$	0,0135
<b>FBPh6</b>	$9,1285 \times 10^{-8}$	815,9516	0,0091
FBPh7	$6,1177 \times 10^{-8}$	234,1968	0,0774
FBDe0	$2,1488 \times 10^{-9}$	3,1715	0,0039
FBDe1	$2,0766 \times 10^{-8}$	46,0572	0,0339
FBDe2	$1,6945 \times 10^{-7}$	871,8633	0,1634
FBDe3	$1,9950 \times 10^{-7}$	$1,4160 \times 10^3$	0,1037
FBDe4	$1,2254 \times 10^{-8}$	114,9180	0,0026
FBDe5	$3,3416 \times 10^{-6}$	$2,2982 \times 10^3$	6,6173
FBDe6	$3,9164 \times 10^{-12}$	0,0335	$7,3169 \times 10^{-7}$
<b>FBDe7</b>	$1,2346 \times 10^{-12}$	0,0014	$2,3195 \times 10^{-6}$
<b>BCFB</b>	$4,0593 \times 10^{-7}$	737,5047	0,6994

**Tab 2.** Mars-Phobos-Deimos Martiocentric errors.

The following plot in Figure 15 compares the binary gravitational parameter  $\mu$  with the  $\Delta V$  required to reach the SOI of Mars by passing in the vicinity of Phobos: it is possible to see how for low values of  $\mu$  the  $\Delta V$  is concentrated around the range centered in 1,2 km/s, a sign that in practice there would be no convenience in implementing a flyby maneuver in the case of the real ternary Mars-Phobos-Deimos system.

As mentioned, the Figure 15 was obtained by sweeping the parameter  $\mu$  in a range from  $1,6606e-8$  to  $1,6606e-1$ , which is why, in order to understand the order of magnitude of the parameter  $\mu$  from which one can appreciate nonnegligible  $\Delta V$  gains, it is necessary to zoom in on the initial part of the graph and, by doing so, it is therefore possible to conclude that the gain in terms of  $\Delta V$  begins to be relevant from a value of  $\mu$  equal to  $3e-3$  onward, since it is from this value that, sporadically, it is possible to begin to have  $\Delta V$  which may be much smaller than the 1,2 km/s of direct escape, and that this advantage gradually becomes more convenient, following a law in which the  $\Delta V$  decreases hyperbolically as the parameter  $\mu$  increases.

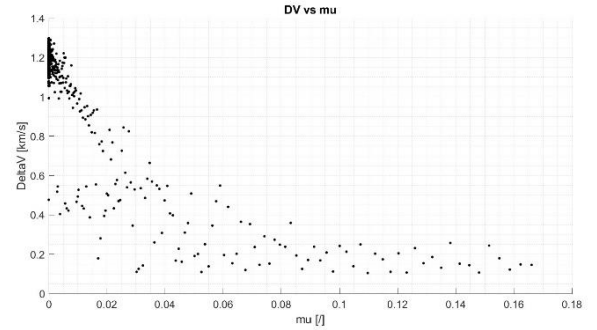


**Figure 15.**  $\Delta V$  vs  $\mu$  plot

## 5. Conclusions

In light of the results obtained and analyzed in the previous chapter, it is possible to draw some very important conclusions, and more importantly, to justify why this analysis was conducted.

The construction of an orbiting station around the Moon emerges as a crucial prospect in the field of space exploration and lunar missions, both because in the first place the Moon is large enough to be able to keep a possible space station on a stable orbit, and because it offers a significant advantage in terms of  $\Delta V$ , allowing a significant reduction in the energy requirements for launching and recovering space missions. Launching a mission from the lunar surface requires a significant amount of energy to overcome lunar gravity and reach lunar orbit. An orbiting station could be placed in a stable and relatively low orbit around the Moon, thus reducing the  $\Delta V$  needed to reach it from a mission from Earth or the Moon itself. This means that less energy is required to reach the orbiting station compared to a direct launch to other deep-space destinations.

Well, by the time mankind succeeds in colonizing Mars, the results obtained show that it is futile to hope that on Phobos and Deimos it makes sense to do something similar, both because they are too small (it would be correct to call them asteroids and not moons, given the size of their radii) and therefore would not be able to maintain a hypothetical space station on a stable orbit around them, and because they would not give any advantage in terms of  $\Delta V$ .

## References

- [1] Jacob A. Dahlke (2018), Optimal Trajectory Generation in a Dynamic Multi- Body Environment using a Pseudospectral Method, Air Force Institute of Technology, Wright-Patterson Air Force Base, Ohio.
- [2] Adam P. Wilmer, Robert A. Bettinger and Bryan D. Little (2021), Preliminary Viability Assessment of CCislunar Periodic Orbits for Space Domain Awareness, Air Force Institute of Technology, Wright-Patterson Air Force Base, Ohio.
- [3] Kenza Boudad, Kathleen Howell, Diane Davis (2021), Energy and Phasing Considerations for Low-Energy Transfers from Cislunar to Heliocentric Space, Purdue University, West Lafayette, Indiana.
- [4] Brian P. McCarthy and Kathleen C. Howell (2021), Quasi-periodic orbits in the Sun-Earth-Moon Bicircular Restricted Four-Body Problem, Purdue University, West Lafayette, Indiana.
- [5] Luigi Mascolo (2023), Low-Thrust Optimal Escape Trajectories from Lagrangian Points and Quasi-Periodic Orbits in a High Fidelity Model, Politecnico di Torino, Turin, Italy.
- [6] Cornelisse J.W., Schöyer, H.F.R., and Wakker, K.F., (1979), Rocket Propulsion and Spaceflight Dynamics, Pitman, London.
- [7] Topputo F. (2013), On Optimal Two-Impulse Earth–Moon Transfers in a Four-Body Model, Politecnico di Milano, Milan, Italy.
- [8] Lorenzo Montana (2021), Ottimizzazione di traiettorie per missioni a flyby multipli con Asteroidi Near-Earth, Politecnico di Torino, Turin, Italy.